

## Solar control of southwest monsoon on centennial timescales

M. Tiwari<sup>1,\*</sup>, R. Ramesh<sup>1</sup>, B. L. K. Somayajulu<sup>1</sup>,  
A. J. T. Jull<sup>2</sup> and G. S. Burr<sup>2</sup>

<sup>1</sup>Physical Research Laboratory, Ahmedabad 380 009, India

<sup>2</sup>NSF Arizona AMS Facility, University of Arizona, Tucson, AZ85721, USA

**Solar forcing is proposed to be a major governing factor for the southwest monsoon (SWM) strength during the Holocene. The southeastern Arabian Sea is significantly affected by monsoon run-off and is an ideal testing ground. We analysed stable oxygen isotopic composition ( $d^{18}\text{O}$ ) of three species of planktonic foraminifera (*Globigerinoides ruber*, *Gs. sacculifer* and *Globarotalia menardii*) with high time-resolution (~50 yrs) in a sediment core raised from the region, and documented past variations in SWM precipitation. High-resolution isotopic and spectral analyses show that solar forcing indeed played a major role in governing the past variations in SWM precipitation on centennial timescales.**

**Keywords:** Arabian Sea, foraminifera, monsoon, stable isotopes, solar forcing.

It has been proposed that earth's climate is sensitive to mild changes in solar output at decadal to millennial timescales<sup>1</sup>. Currently, there has been renewed interest in climate forcing by Total Solar Irradiance (TSI), which shows remarkable agreement with the smoothed global temperature of the 20th century<sup>2</sup>. Precise measurement of TSI has been made using space-borne radiometers; it varies with an rms amplitude of about 0.1% in response to the changing area covered by sunspots on the solar disk. But this variation seems to be too low to cause widespread climatic change. It could be that there is a large amplitude, slowly varying component of TSI, overlooked by the space-borne measurements. It is believed that TSI might have been lower by as much as 0.25% during the Maunder Minimum (AD ~ 1700) than at present<sup>3</sup> and even a minor variation in TSI (0.1–0.3%) could bring about major changes in monsoonal precipitation via various positive feedback processes, such as moisture availability and changes in atmospheric circulation<sup>1,4,5</sup>. Neff *et al.*<sup>4</sup> measured stable oxygen isotope ratios ( $d^{18}\text{O}$ , monsoon proxy) in Oman speleothems for the period 9 to 6 ka and compared them with  $\Delta^{14}\text{C}$  values from tree rings, which are dependent on cosmic ray fluxes modulated by solar activity. They found excellent correlation between the monsoon and solar activity proxies and proposed that variation in solar radiation has a prominent control over the monsoon on centennial to decadal timescales. Fleitmann *et al.*<sup>6</sup> analysed Holocene stalagmites from Oman and compared  $d^{18}\text{O}$  data with

GRIP ice core  $d^{18}\text{O}$  and  $\Delta^{14}\text{C}$  records from tree rings. They proposed that early Holocene monsoon circulation was controlled by glacial boundary conditions such as northward heat transport in the Atlantic and thermohaline circulation. Subsequently, after 8 ka, as the thermohaline circulation stabilized, the monsoon circulation responded more directly to solar forcing<sup>6</sup>. Agnihotri *et al.*<sup>7</sup> obtained a core from the northeastern Arabian Sea, off the Gujarat coast and analysed it for three palaeoclimatic proxies (organic carbon, nitrogen and aluminum content of marine sediments) for the past 1200 years and compared them with TSI data. They found nearly similar trends for these proxies and TSI variation within the radiocarbon dating errors; lower TSI was accompanied by lower productivity and reduced run-off, indicating weakened SWM. Spectral analyses of the TSI, palaeoclimatic proxies and SWM rainfall yielded similar periodicities, which led them to infer that solar forcing controlled the monsoonal precipitation on multi-decadal timescales<sup>7,8</sup>, similar to the results obtained on varve sediments off Karachi<sup>9</sup>. They<sup>7</sup> reported weight % and not the burial fluxes; these proxies reflect the strength of the SWM wind and not precipitation. The southeastern Arabian Sea offers an opportunity to determine the past fluctuations in precipitation, as it receives freshwater run-off during the SW monsoon<sup>10</sup>. We carried out high-resolution oxygen isotope analysis of planktonic foraminifera from a sediment core in the region, which documents past variations in SW monsoon precipitation.

The core is from the eastern continental margin of the Arabian Sea (12.6°N, 74.3°E; water depth = 400 m; dated length = 252 cm) off Mangalore coast (Figure 1). This core (SK145-9) has eleven dates covering ~13,000 calendar years (spanning 252 cm length) providing an average sedimentation rate of 19 cm/10<sup>3</sup> years (Table 1). It has an average resolution of ~50 years per cm. The top 50 cm has been sampled at every centimere and below 50 cm sampling was done at every 2 cm. The top 50 cm of this core (sampled closely), covering a time span of approximately 2800 years (Figure 2), has been taken for further studies. Thus it offers a high time-resolution and therefore will aid in under-

**Table 1.** Uncalibrated and calibrated AMS radiocarbon ages of planktonic foraminifera for core SK145-9. Errors quoted are 1 $\sigma$

Depth (cm)	Radiocarbon age (yrs BP)	Calibrated age (yrs BP)
0–2	844 ± 36	410 ± 80
23–25	1899 ± 56	1330 ± 80
40–41	2506 ± 39	2030 ± 70
50–52	3210 ± 41	2860 ± 70
78–80	3952 ± 53	3820 ± 80
124–126	6308 ± 48	6650 ± 60
160–162	8124 ± 66	8450 ± 90
174–176	8891 ± 64	9210 ± 270
210–212	9359 ± 57	9840 ± 230
228–230	9922 ± 58	10430 ± 380
250–252	11913 ± 73	13180 ± 350

\*For correspondence. (e-mail: tmanish@prl.res.in)

standing sub-centennial scale variability. The top of the core (viz. 0–2 cm) has a calibrated age of  $410 \pm 80$  yrs. Radiocarbon dates in this core have been converted to calendar ages using the calibration program Calib 4.1 (INTCAL 98)<sup>11</sup>, with a reservoir age correction of  $500 \pm 30$  yrs (deviation from the assumed value of 400 yrs, i.e.  $\Delta R = 100 \pm 30$  yrs)<sup>12,13</sup>.

For oxygen isotope analyses, 30–35 shells of the three species of planktonic foraminifera, viz. *Globigerinoides ruber*, *Gs. sacculifer*, and *Globorotalia menardii* were handpicked and analysed using GEO 20-20 mass spectrometer (Europa Scientific, UK) at Physical Research Laboratory, Ahmedabad, India. The size range chosen for separating bulk foraminifera was 250–500  $\mu\text{m}$ , but while picking foraminifera care was taken to pick the shells falling approximately in the range 350–450  $\mu\text{m}$ . The external precision on  $d^{18}\text{O}$  measurement is better than  $\pm 0.1\text{‰}$  (1 $\sigma$  standard deviation) as determined by the three daily measurements of an internal calcitic standard (standard error is 0.02‰). All isotopic values are reported with respect to V-PDB. Further experimental details can be found elsewhere<sup>14</sup>.

During SWM, abundant precipitation takes place over the Western Ghats (up to 4000 mm/yr)<sup>10</sup> that lie parallel to the western Indian coast from  $\sim 20$  to  $\sim 10^\circ\text{N}$  latitude. This freshwater quickly runs off to the coastal Arabian Sea and reduces the sea surface salinity considerably. Along the southwestern Indian coast, the salinity contours become north-south with low salinities of up to 34 PSU pointing towards the freshwater influx and away from the coast, salinity rapidly increases, reaching up to 36 PSU<sup>15</sup> (Figure 1).

Oxygen isotopic data on three species of foraminifera are shown in Figure 3. *Gs. ruber* and *Gs. sacculifer* are surface-dwelling species predominantly inhabiting the top 25 and 50 m respectively, whereas *Gr. menardii* is a deeper-dwelling species<sup>16–18</sup>, predominantly inhabiting 100–150 m. Thus an oxygen isotope signal arising due to any surface

processes (e.g. salinity change) will be most pronounced in the surface-dwelling species, viz. *Gs. ruber* and *Gs. sacculifer* and will be subdued in the deeper-dwelling species, i.e. *Gr. menardii*. *Gs. ruber* is a warm-water species with maximum abundance at  $\sim 25^\circ\text{C}$  SST and salinity range of 36–37 PSU. It is most abundant in the subtropical regions, with relative abundances<sup>19</sup> reaching up to 35–40%. *Gs. sacculifer* is a tropical water species with maximum abundance at  $28^\circ\text{C}$  and salinity of 36 PSU. This species has a preference for water masses with low seasonality (i.e. difference between summer and winter conditions) in SST and vertical temperature gradient<sup>19</sup>. *Gr. menardii* is a species most abundant in the equatorial and tropical regions with clear preference to warm waters ( $\sim 28^\circ\text{C}$  SST) and a salinity<sup>19</sup> of  $\sim 35$  PSU.

Factors controlling the oxygen isotopes in foraminiferal shells are the sea surface salinity (SSS) and SST<sup>20</sup>. For the past  $\sim 3$  ka, there has been no salinity fluctuations due to the global ice-volume effect, as there were no significant global ice-melting episodes affecting the sea level<sup>21</sup>. Moreover, SST variations in the tropics for the past 10 ka are very small ( $\sim 0.5^\circ\text{C}$ ) and negligible<sup>22</sup> for the past 3 ka. The studied species are known to grow predominantly during SWM and hence are likely to record signals arising mainly due to SWM fluctuations<sup>23</sup>. In the eastern Arabian Sea, SSS variation is mainly controlled by a variation in the supply of freshwater as surface run-off from the adjacent Western Ghats during SWM. This freshwater acts as a lid and prevents vertical mixing (upwelling) due to monsoon winds<sup>24–26</sup>. We therefore assume that the dominant factor controlling the  $d^{18}\text{O}$  signals in the eastern Arabian Sea is

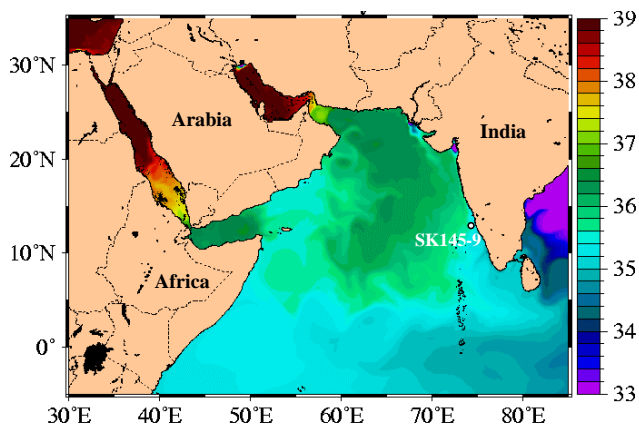


**Figure 1.** Location of core SK145-9 (shown by white circle). Surface salinity contours in the Arabian Sea during September<sup>15</sup> (unit is PSU). Note that in the eastern Arabian Sea, salinity is low along the southwestern coast of India (adjacent to the Western Ghats) and increases rapidly towards the open ocean.

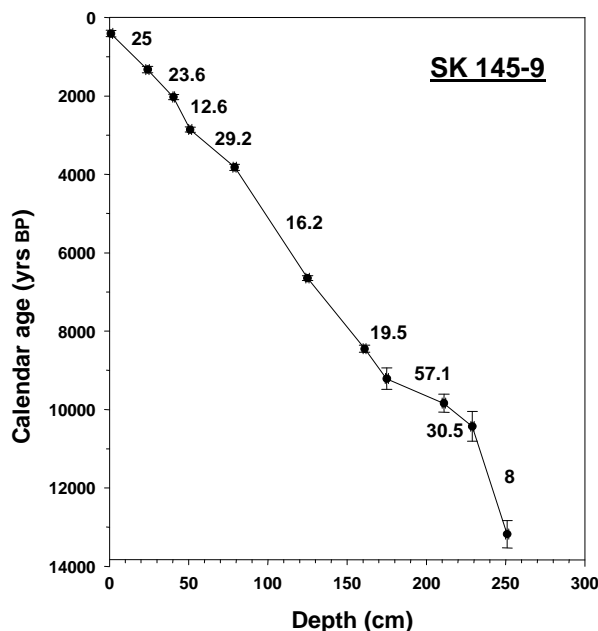


**Figure 2.** Calibrated radiocarbon ages and sedimentation rates (cm/ka) for various intervals in the core SK145-9. Errors quoted are 1 $\sigma$ .

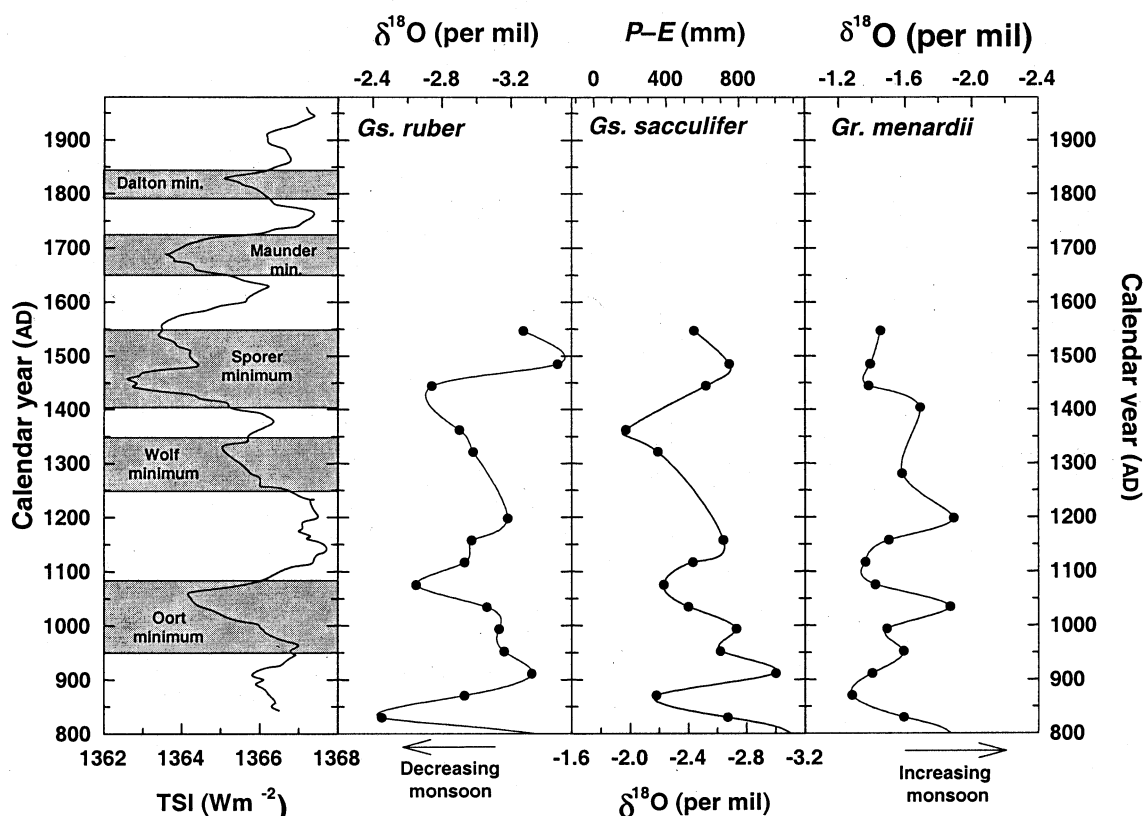


**Figure 3.** Comparison of TSI data and precipitation proxies ( $d^{18}O$  of three species of foraminifera viz. *Gs. ruber*, *Gs. sacculifer* and *Gr. menardii*) for the past 1200 years (radiocarbon dating error is  $\pm 80$  yrs). Thick line in the first panel depicts 10-year running average of splined data showing centennial scale variations. Top of third panel indicates precipitation–evaporation calculated using an empirical equation (see text).

the SSS change induced by the variation in SWM precipitation; for every per mil decline in salinity, the  $d^{18}O$  value decreases<sup>10,27</sup> by 0.33‰. Thus a depleted  $d^{18}O$  signal indicates enhanced SWM precipitation, whereas an enriched  $d^{18}O$  signal points towards reduced precipitation due to weaker SWM. One might argue that there may be some effect of SST changes due to upwelling; if so, the difference between the  $d^{18}O$  values of *Gs. ruber* and *Gs. sacculifer* should be close to zero (both will be equally affected by upwelling). But this is not the case and *Gs. ruber* values are always depleted compared to *Gs. sacculifer* values by a mean of 0.52‰.

To obtain a quantitative estimate of the rainfall variation over the southeastern coastal Arabian Sea, a parameter  $P-E$ , i.e. excess of precipitation over evaporation has been approximately estimated. Ramesh Kumar and Prasad<sup>28</sup> calculated  $P-E$  values for this region during the monsoon season using temperature, salinity and wind stress as the primary data. The core top  $d^{18}O$  values of *Gs. sacculifer* (predominantly inhabits top  $\sim 50$  m and major growing season is during SWM) have been calibrated with the  $P-E$  data and an approximate transfer function has been obtained<sup>29</sup> for the eastern Arabian Sea:

$$P-E \text{ (mm)} \sim -800d^{18}O - 1400.$$

The  $P-E$  values are depicted at the top of third panel of Figure 3. As evident from Figure 3, the values fluctuate between a minimum of  $\sim 175$  mm and a maximum of  $\sim 1000$  mm.

We use reconstructed TSI data for the past 1200 years of Bard *et al.*<sup>30</sup>, based on the common fluctuations of the  $^{14}C$  and  $^{10}Be$  production rates obtained from tree rings and polar ice sheets. The TSI curve assumes a 0.25% reduction in TSI during Maunder Minimum<sup>3</sup>. The data are unequally spaced at 8 to 10 year intervals, which is first splined for every ten-years and then a ten-point running average is taken so that resolution of the TSI data becomes comparable that for isotope data of core SK 145-9. TSI data are then compared with  $d^{18}O$  in all the three foraminiferal species, which is a more robust proxy for SWM precipitation (Figure 3, productivity proxies such as sedimentary  $CaCO_3$  and organic carbon content cannot be used in this region, as their relationship with SWM is complicated).

The core SK 145-9 does not extend beyond AD 1550 and TSI data are available from AD 850 onwards only; hence comparison can be made for only seven centuries. As evident from Figure 3, precipitation signals from all the three species match reasonably well with the TSI fluctuations within the radiocarbon age uncertainties ( $\sim 80$  yrs). Exact matching is not seen between precipitation and TSI sig-

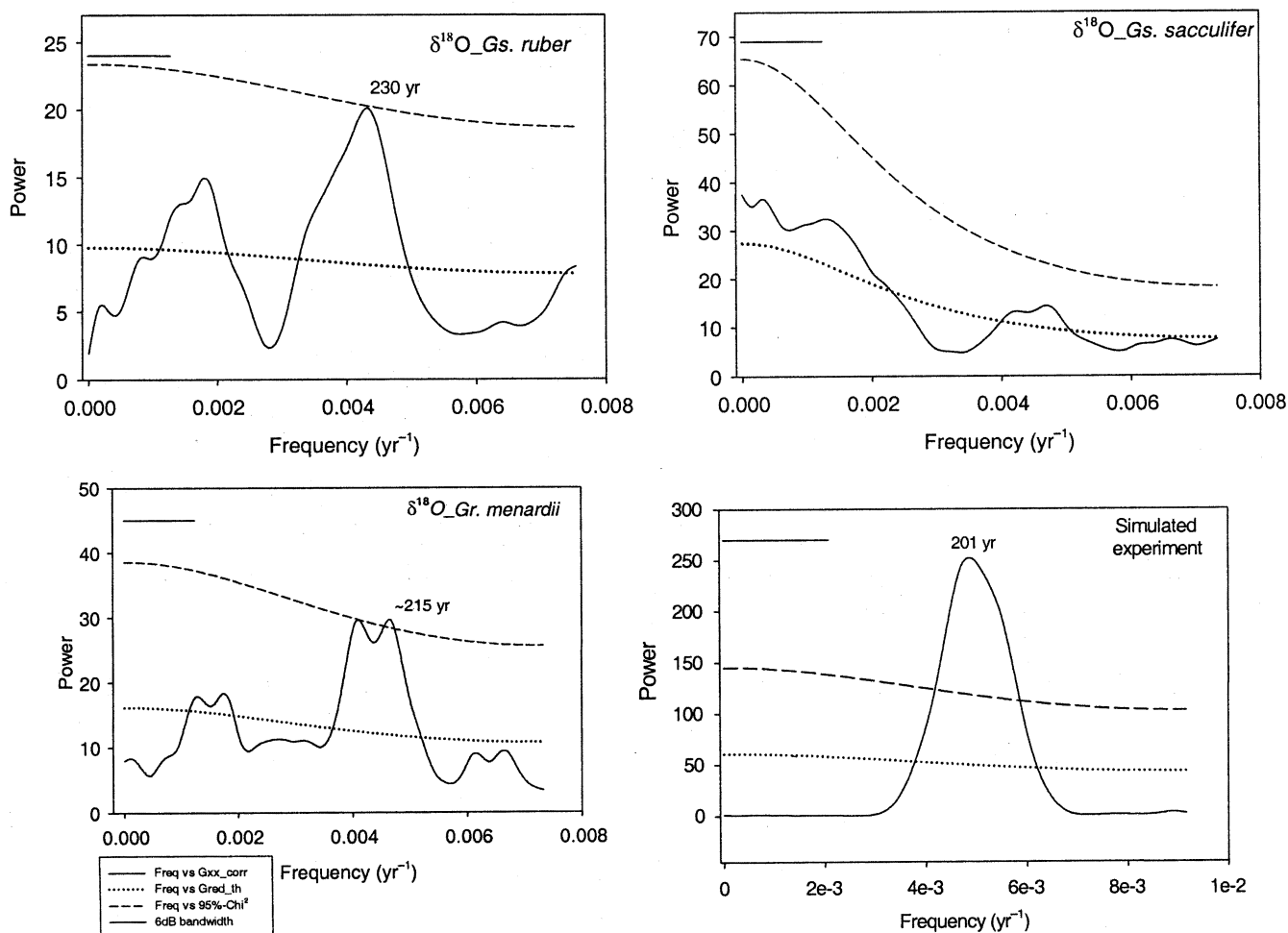


**Figure 4.** Power spectra of oxygen isotope time series of three species of foraminifera and the simulated experiment. Horizontal line at the upper left-hand corner represents 6 dB bandwidth of spectral resolution. Gxx\_corr denotes amplitude or power of various frequencies; Gred\_th shown by dotted line is the background signal; dashed line denotes 95% significance level calculated using the chi-square test.

nals, which could be due to coarser resolution of the sedimentary record compared to that of TSI. In general, during periods of lower TSI values, we get lower precipitation implying a solar forcing on SWM precipitation on centennial timescales. During the periods of reduced solar irradiance, viz. Oort, Wolf and Spörer minima, precipitation reduces as indicated by enhanced  $d^{18}\text{O}$  values. Thus our study reinforces the earlier findings of Agnihotri *et al.*<sup>7</sup> from elsewhere in the Arabian Sea.

Spectral analysis can possibly help in delineating the factors forcing the monsoon. Spectral analysis has been carried out on the oxygen isotope time series of all the three species of foraminifera for the past ~2900 years (37 data points each) using REDFIT 3.6 program (Figure 4)<sup>31</sup>. The  $d^{18}\text{O}$  in *Gr. menardii* exhibits a significant periodicity of ~215 yrs and in *Gs. ruber* it shows a periodicity of ~230 yrs, which is just below the 95% significance level. This points towards the fact that SWM follows a dominant quasi periodicity, of ~200 yrs, which is similar to that of the 200-yr Suess solar cycle<sup>32</sup>. In the case of *Gs. saccu-*

*lifer*, all the frequencies are suppressed and well below the 95% significance level.

Earlier, ~200, 113, ~77 and ~53 yrs periodicities have been observed in the TSI data<sup>7</sup>. Furthermore, power spectra of various proxies controlled by monsoon strength in a core from the northeastern Arabian Sea<sup>7</sup>, show significant periodicities of ~200, ~110 and 56 yrs. A recent high-resolution study on a 9000 yr long speleothem from southern China has revealed prominent periodicities of 558, 206, 159, 24, 22–17, 16–15 years in Asian monsoon<sup>33</sup>. Most of these periodicities match with that obtained on the  $\Delta^{14}\text{C}$  (controlled by solar activity), which reinforces the hypothesis that the intensity of Asian monsoon is affected by variations in solar activity<sup>33,34</sup>. Lower frequencies are not observed in our study due to the average sample resolution, which is ~65 yrs. This along with the periodicities observed in our study, indicates that SWM intensity on a centennial scale is governed by variation in TSI. *Gs. sacculifer* responds differently in the power spectrum, possibly because the range of variation of its

$d^{18}\text{O}$  is higher than that of *Gs. ruber*, as indicated by the higher magnitude of power (y-axis). This might be due to the vertical migration in the water column of *Gs. sacculifer*.

To check the effect of discrete sampling and dating uncertainty on the periodicity obtained from power spectral analysis, we carried out the following experiment. We generated a 3000 yr long time series with a periodicity of 200 yrs  $\{y = \sin(2\pi t/200)\}$  and sampled it with 50 yr resolution (60 data points). We chose four time values and assigned them random errors ( $\pm 80$  yrs) corresponding to the radiocarbon dating uncertainty. Then we used the 'dates' and assigned time for each datum point by interpolation. This dataset was then used to obtain the power spectrum. We retrieved a period of  $\sim 201$  yrs with an error of 50 yrs (Figure 4). This was significant at 95% confidence level. Thus the effect of discrete sampling and dating uncertainty is less than 50 yrs for the obtained periodicities.

Spectral analysis and visual matching of the high-resolution isotopic data from a region best suited to study SWM precipitation with TSI reconstruction, indicates a possible solar control over SWM on centennial timescales. Variations in TSI ( $\sim 0.2\%$ ) seem to be too small to perturb the SWM, unless assisted by some internal amplification mechanism with positive feedback.

Two such mechanisms have been proposed. The first involves heating of the earth's stratosphere by increased absorption of solar ultraviolet (UV) radiation by ozone during periods of enhanced solar activity<sup>35</sup>. It is known that the magnitude of variation in UV is higher than that in TSI. The positive feedback is that more the UV, more the ozone production and more the heating. This heating is transferred to the troposphere as shown by theoretical models<sup>36</sup>. Enhanced heating results in increased thermal contrast between the Asian land mass and the Indian Ocean, and also increases evaporation from the oceans, thus enhancing the monsoon winds and precipitation. This involves another possible feedback: release of latent heat to the troposphere by monsoon precipitation, which in turn strengthens the monsoon winds.

The second mechanism is that during periods of higher solar activity, the flux of galactic cosmic rays to the earth is reduced, providing less cloud condensation nuclei, resulting in less cloudiness<sup>35,36</sup>. This extra heating of the troposphere increases the evaporation from the oceans.

The common periodicities exhibited both by the precipitation proxy (oxygen isotope of planktonic foraminifera) and TSI corroborate our inference that SWM precipitation is governed by a solar variability on centennial timescales, even though the exact linking mechanism is yet to be elucidated.

1. Bond, G. *et al.*, Persistent solar influence on North Atlantic climate during the Holocene. *Science*, 2001, **294**, 2130–2136.
2. Foukal, P., Can slow variation in solar luminosity provide missing link between the sun and climate? *EOS*, 2003, **84**, 205–208.

3. Lean, J., Beer, J. and Bradley, R., Reconstruction of solar irradiance since 1610: Implications for climatic change. *Geophys. Res. Lett.*, 1995, **22**, 3195–3198.
4. Neff, U., Burns, S. J., Mudelsee, M., Mangini, A. and Matter, A., Strong coherence between solar variability and the monsoon in Oman between 9 and 6 kyrs ago. *Nature*, 2001, **411**, 290–293.
5. Mehta, V. and Lau, K. M., Influence of solar irradiance on the Indian monsoon-ENSO: Relationship at decadal-multidecadal timescales. *Geophys. Res. Lett.*, 1997, **24**, 159–162.
6. Fleitmann, D., Burns, S. J., Mudelsee, M., Neff, U., Kramers, J., Mangini, A. and Matter, A., Holocene forcing of the Indian monsoon recorded in a stalagmite from southern Oman. *Science*, 2003, **300**, 1737–1739.
7. Agnihotri, R., Dutta, K., Bhushan, R. and Somayajulu, B. L. K., Evidence for solar forcing on the Indian monsoon during the last millennium. *Earth Planet. Sci. Lett.*, 2002, **198**, 521–527.
8. Agnihotri, R. and Dutta, K., Centennial scale variations in monsoonal rainfall (Indian, east equatorial and Chinese monsoons): Manifestations of solar variability. *Curr. Sci.*, 2003, **85**, 459–463.
9. von Rad, U., Schaaf, M., Michels, K. H., Schulz, H., Berger, W. H. and Sirocko, F., A 5000-yr record of climate change in varved sediments from the oxygen minimum zone off Pakistan, northeastern Arabian Sea. *Quat. Res.*, 1999, **51**, 39–53.
10. Sarkar, A., Ramesh, R., Somayajulu, B. L. K., Agnihotri, R., Jull, A. J. T. and Burr, G. S., High resolution Holocene monsoon record from the eastern Arabian Sea. *Earth Planet. Sci. Lett.*, 2000, **177**, 209–218.
11. Stuiver, M. *et al.*, INTCAL98 radiocarbon age calibration, 24,000–0 cal BP. *Radiocarbon*, 1998, **40**, 1041–1083.
12. Dutta, K., Bhushan, R. and Somayajulu, B. L. K.,  $\Delta R$  correction values for the northern Indian Ocean. *Radiocarbon*, 2001, **43**, 483–488.
13. Southon, J., Kashgarian, M., Fontugne, M., Metivier, B. and Yim, W-S Wyss, Marine reservoir corrections for the Indian Ocean and Southeast Asia. *Radiocarbon*, 2002, **44**, 167–180.
14. Ramesh, R. and Tiwari, M., Significance of stable oxygen ( $d^{18}\text{O}$ ) and carbon ( $d^{13}\text{C}$ ) isotopic compositions of individual foraminifera (*O. universa*) in a sediment core from the eastern Arabian Sea. In *Micropaleontology: Application in Stratigraphy and Paleoceanography* (ed. Sinha, D. K.), Narosa Publ., New Delhi, 2005, pp. 309–329.
15. Naval Research Laboratory, United States Navy website; [www7320.nrlssc.navy.mil/global\\_ncom/ara.html](http://www7320.nrlssc.navy.mil/global_ncom/ara.html)
16. Bè, A. W. H., An ecological, zoogeographic and taxonomic review of recent planktonic foraminifera. In *Oceanic Micropaleontology* (ed. Ramsey, A. T. S.), Academic Press, London, 1977, pp. 1–100.
17. Fairbanks, R. G., Wiebe, P. H. and Bè, A. W. H., Vertical distribution and isotopic composition of living planktonic foraminifera in the western North Atlantic. *Science*, 1980, **207**, 61–63.
18. Fairbanks, R. G., Sverdrlove, M., Free, R., Wiebe, P. H. and Bè, A. W. H., Vertical distribution and isotopic fractionation of living planktonic foraminifera from the Panama basin. *Nature*, 1982, **298**, 841–844.
19. Hilbrecht, H., Extant planktic foraminifera and the physical environment in the Atlantic and Indian Oceans. Mitteilungen aus dem Geologischen Institut der Eidgen. Technischen Hochschule und der Universität Zürich, Neue Folge. Zürich, 1996, No. 300, 93 pp. (web address: [http://www.fuhrmann-hilbrecht.de/Heinz/geology/HH1996/aa\\_start.html](http://www.fuhrmann-hilbrecht.de/Heinz/geology/HH1996/aa_start.html)).
20. Shackleton, N. J., Oxygen isotope analyses and Pleistocene temperatures reassessed. *Nature*, 1967, **215**, 15–17.
21. Fairbanks, R. G., A 17,000-year glacio-eustatic sea level record: Influence of glacial melting rates on the Younger Dryas event and deep ocean circulation. *Nature*, 1989, **342**, 637–642.
22. Rostek, F., Ruhland, G., Bassinot, F. C., Muller, P. J., Labeyrie, L. D., Lancelot, Y. and Bard, E., Reconstructing sea surface tempera-

- ture and salinity using  $d^{18}O$  and alkenone records. *Nature*, 1993, **364**, 319–321.
23. Guptha, M. V. S., Curry, W. B., Ittekkot, V. and Murlinath, A. S., Seasonal variation in the flux of planktic foraminifera: Sediment trap results from the Bay of Bengal, Northern Indian Ocean. *J. Foraminiferal Res.*, 1997, **27**, 5–19.
  24. McCreary, J. P., Kundu, P. K. and Molinari, R. L., A numerical investigation of dynamics, thermodynamics and mixed layer processes in the Indian Ocean. *Prog. Oceanogr.*, 1993, **31**, 181–224.
  25. Shankar, D. and Shetye, S. R., On the dynamics of the Lakshadweep high and low in the southeastern Arabian Sea. *J. Geophys. Res.*, 1997, **102**, 12551–12562.
  26. Thamban, M., Rao, V. P., Schneider, R. R. and Grootes, P. M., Glacial to Holocene fluctuations in hydrography and productivity along the southwestern continental margin of India. *Palaeogeogr. Palaeoclimatol. Palaeoecol.*, 2001, **165**, 113–127.
  27. Duplessy, J. C., Bè, A. W. H. and Blanc, P. L., Oxygen and carbon isotopic composition of planktonic foraminifera in the Indian Ocean. *Palaeogeogr. Palaeoclimatol. Palaeoecol.*, 1981, **33**, 9–46.
  28. Ramesh Kumar, M. R. and Prasad, T. G., Report, NIO/TR-4/95, National Institute of Oceanography Goa, 1995, pp. 9–46.
  29. Ramesh, R., High resolution Holocene monsoon records from different proxies: An assessment of their consistency. *Curr. Sci.*, 2001, **81**, 1432–1436.
  30. Bard, E., Raisbeck, G., Yiou, F. and Jouzel, J., Solar irradiance during the last 1200 years based on cosmogenic nuclides. *Tellus B*, 2000, **52**, 985–992.
  31. Schulz, M. and Mudelsee, M., Estimating red-noise spectra directly from unevenly spaced palaeoclimatic time series. *Comput. Geosci.*, 2002, **28**, 421–426.
  32. Usoskin, I. G. and Mursula, K., Long-term solar cycle evolution: Review of recent developments. *Sol. Phys.*, 2003, **218**, 319–343.
  33. Wang, Y. *et al.*, The Holocene Asian monsoon: Links to solar changes and North Atlantic climate. *Science*, 2005, **308**, 854–857.
  34. Kerr, R. A., Changes in the sun may sway the tropical monsoon. *Science*, 2005, **308**, 787.
  35. Schneider, D., Living in sunny times. *Am. Sci.*, 2005, **93**, 22–24.
  36. Friis-Christensen, E. and Svensmark, H., What do we really know about the sun–climate connection? *Adv. Space Res.*, 1997, **20**, 913–921.

ACKNOWLEDGEMENTS. We thank the Indian Space Research Organization Geosphere Biosphere Programme for funding, and G. J. Reichart for constructive suggestions.

Received 4 April 2005; revised accepted 1 August 2005

## Presence/role of twin gyres in the El Nino 3.4 domain

P. Rahul Chand Reddy\* and P. S. Salvekar

Indian Institute of Tropical Meteorology, Pune 411 008, India

**El Nino is the ‘weather pulse’ of the world climate, arising out of the interactions between ocean and atmosphere. In the ocean, it is caused and cushioned by the interaction of the Kelvin and Rossby waves, but the mode/method and the consequences of their interaction are still not clear. It has been shown in the Indian Ocean that such interference results in a system of westward propagating equatorial twin gyres<sup>1</sup>. By analysing the surface circulations of a global model (MIT-OGCM) as well from WOCE, TOPEX SSHs, TAO and AVHRR SSTs, we report a similar feature of the Pacific twin gyres along the equator in the El Nino domain, especially in the Nino 3.4 domain (170°E–120°W, 10°S–10°N). The possible role of these eddies in inducing warmer temperatures with reference to the El Nino period is investigated.**

**Keywords:** El Nino, Kelvin and Rossby waves, Pacific Ocean, sea surface temperature, twin gyres.

EL Nino is one of the most striking examples of inter-annual climate variability on a global scale. Tropical Ocean and Global Atmosphere (TOGA)<sup>2,3</sup> coupled with numerical/modelling studies<sup>4–10</sup> have improved our understanding of the El Nino Southern Oscillation (ENSO). Several mechanisms are responsible for the rapid horizontal redistribution of heat in the upper ocean in response to the relaxation of winds over the Pacific Ocean during ENSO. The existence of ENSO is attributed to the dynamic coupling between the atmosphere and ocean in the equatorial Pacific region. This dynamic coupling refers to the positive feedback loop among the surface wind stress, sea surface temperature (SST) gradients and ocean upwelling. Since upwelling is driven by surface winds, changes in the strength of the surface winds affect the strength of upwelling, which in turn affects the SST gradients. Deepening of the thermocline to the east along the equatorial Pacific during El Nino is attributed to change in the easterly wind patterns reflecting on the upwelling and subsequently on the SSTs.

It is interesting to note from this study that during El Nino, the excited Kelvin waves suppress the Rossby waves. However, the deepening in the thermocline, specially towards the east owes its existence to the gyres that evolve following the interaction between the Kelvin and reflected Kelvin [Rossby] waves. It is often noticed that in the El Nino 3.4 domain, the sea surface height (SSH) and SST are slightly higher on the north of the equator than on the south. This could be attributed to the anticyclonic circulation

\*For correspondence. (e-mail: irsp4@yahoo.co.in)